

# Microstructural Characteristics and Mechanical Properties of Dissimilar Joints of AISI 316LN Austenitic Stainless Steel and Modified 9cr-1Mo Steel

K. Karthick<sup>1</sup>, S. Malarvizhi<sup>2</sup>, V. Balasubramanian<sup>3</sup>, S. A. Krishnan<sup>4</sup>, G. Sasikala<sup>5</sup> and Shaju K. Albert<sup>6</sup>

<sup>1</sup> Research Scholar, Centre for Materials Joining and Research, Department of Manufacturing Engineering, Annamalai University, Annamalai Nagar - 608 002, Tamil Nadu, India.  
Email: karthick.kuppan@gmail.com (Corresponding Author)

<sup>2</sup> Associate Professor, Centre for Materials Joining and Research, Department of Manufacturing Engineering, Annamalai University, Annamalai Nagar – 608 002, Tamil Nadu, India. Email: jeejoo@rediffmail.com

<sup>3</sup> Professor & Director, Centre for Materials Joining and Research, Department of Manufacturing Engineering, Annamalai University, Annamalai Nagar – 608 002, Tamil Nadu, India. Email: visvabalu@yahoo.com

<sup>4</sup> Scientific Officer - E, Homi Bhabha National Institute, Indira Gandhi Centre for Atomic Research, Kalpakkam - 603 102, Tamil Nadu, India. Email: sakrish@igcar.gov.in

<sup>5</sup> Scientific Officer - H<sup>+</sup>, Homi Bhabha National Institute, Indira Gandhi Centre for Atomic Research, Kalpakkam - 603 102, Tamil Nadu, India. Email: gsasi@igcar.gov.in

<sup>6</sup> Scientific Officer - H<sup>+</sup>, Homi Bhabha National Institute, Indira Gandhi Centre for Atomic Research, Kalpakkam - 603 102, Tamil Nadu, India. Email: shaju@igcar.gov.in



DOI : 10.22486/iwj/2017/v50/i4/162273

## ABSTRACT

In liquid metal cooled fast breeder reactors, the dissimilar joint between grade 91 ferritic steel and 316LN stainless steel is frequently encountered. For better integrity assessment, mechanical properties of each region need be evaluated. In the present investigation, dissimilar joints between grade 91 to 316LN SS were fabricated by shielded metal arc welding process using nickel based electrodes. Mechanical properties (Tensile and impact toughness) of different regions were evaluated by placing the notch at each location. Microhardness variation across the dissimilar joint was recorded. Microstructural analyses of various regions were done by optical and scanning electron microscopy. From this investigation, it is understood that the in-homogeneous mechanical properties were observed across the dissimilar joint. The development of complex microstructure at the fusion interfaces will alter the mechanical properties across the dissimilar joint.

**KEYWORDS :** Welding; Dissimilar joint; Mechanical properties; Microstructure; Microhardness.

## 1.0 INTRODUCTION

In liquid metal cooled fast breeder reactors, grade 91 ferritic steel and 316LN stainless steel are the potential material for steam generators and primary heat exchanger systems. So, the dissimilar joint between grade 91 to 316LN is inevitable. In earlier days, stainless steel electrodes were used to join these materials but it resulted in early failures due to thermal stress mismatch, carbon migration and sigma phase formation [1]. To

minimize these problems, Nickel based (Inconel 82 and Inconel 182) consumables are used because the thermal expansion of this material (15.5  $\mu\text{m}/\text{m}/^\circ\text{C}$ ) lies in-between to the P91 (12.8  $\mu\text{m}/\text{m}/^\circ\text{C}$ ) and 316LN (18  $\mu\text{m}/\text{m}/^\circ\text{C}$ ). Also, these consumables have significantly retarded the carbon migration. In dissimilar joint, the strength and toughness properties of each region will be different because of physical and chemical mismatch between base metals and filler metals [2]. This mismatch states will affect the failure behavior of DMJ.

For the reliable structural integrity assessment, one should know the strength and toughness properties of each region. So far, many authors [3-5] reported the mechanical property variations in each region of DMJ by using miniature tensile specimens but the results reported by them is not accurate because it is case-dependent results. Also, miniature tensile specimens will yield higher elongations compared to standard size specimens. To avoid the above problems, notched cross weld tensile test has been proposed in this investigation. Generally, transverse tensile test is extensively used in industries to qualify welds [6], i.e. the failure occurs in the base metal that represents a good scenario, or in the weld metal or HAZ that is often not wanted. Due to the notch, plastic deformation is forced to develop at the root of the notch and failure occurs due to stress concentration effect. In this investigation, notch tensile properties of different regions of DMJ was evaluated by placing the notch at the desired locations and the impact toughness variations are also calculated by using standard Charpy V-notch specimens. Microhardness test is also conducted to identify the weakest region of DMJ and the characterization of different regions was reported in this paper.

**2.0 EXPERIMENTAL**

Rolled plates of grade 91 ferritic steel and 316 LN SS were used in this investigation. The dissimilar joints were fabricated by shielded metal arc welding process using K-joint configuration. Before welding, the grade 91 ferritic steel was buttered with Inconel 182 electrodes with a heat input of 0.56 kJ/mm. After this, a normal welding between grade 91 and 316 LN were employed. The heat input was varied between 0.48-0.76 kJ/mm. The notch tensile and impact toughness specimens were extracted from various regions of dissimilar joints through EDM process. The scheme of extraction of specimens is shown in Fig. 1. The dimensions of tensile and impact specimens are shown in Fig. 2. Microhardness variations across the DMJ were carried out using Vicker's microhardness tester.

The load and distance between two indentations are 100g and 0.2mm respectively. Microstructural characteristics of DMJ were carried out by using the light optical microscope.

The fractured surfaces of tensile and impact specimens were analyzed under scanning electron microscope.

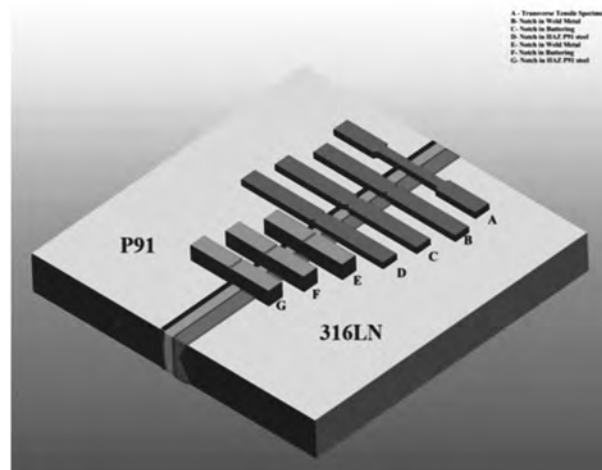


**Fig. 1 : Extraction of specimens**

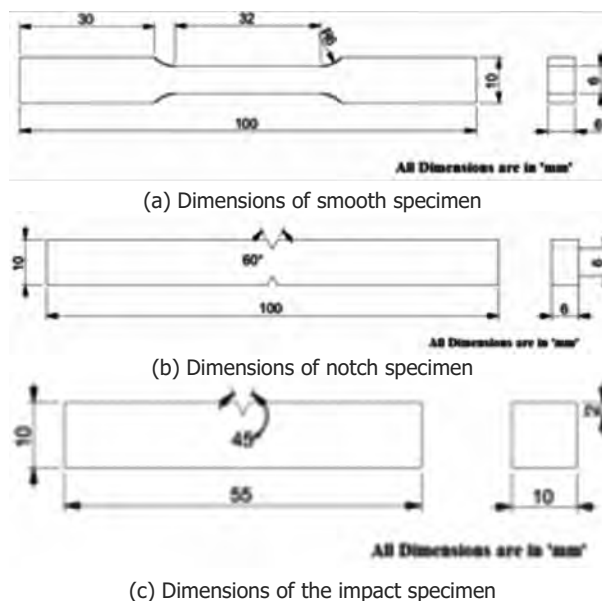


**Fig. 2 (a-c). Dimensions and photographs of tensile and impact specimens**

**3. RESULTS AND DISCUSSION**

**3.1 Macro and Microstructure**

The optical micrographs of base metals are shown in Fig. 3. The grade 91 ferritic steel contains tempered martensitic structure along with the second phase particles. Jones et al. [7] reported that these secondary phase particles belong to  $M_{23}C_6$  and  $V_4C_3$  type carbides which form during tempering (760 °C for 2h) of the base metal and also increases high temperature tensile and creep strength. The micrograph of SS 316LN comprise of fully equiaxed austenite grains.

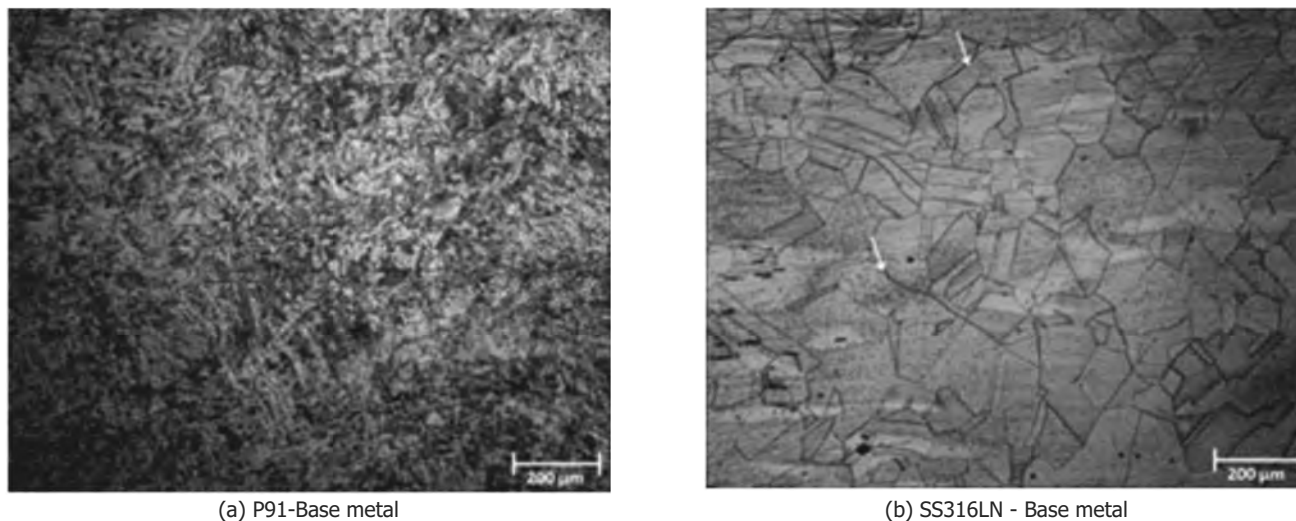


**Fig. 3 : Optical micrographs of base metals**

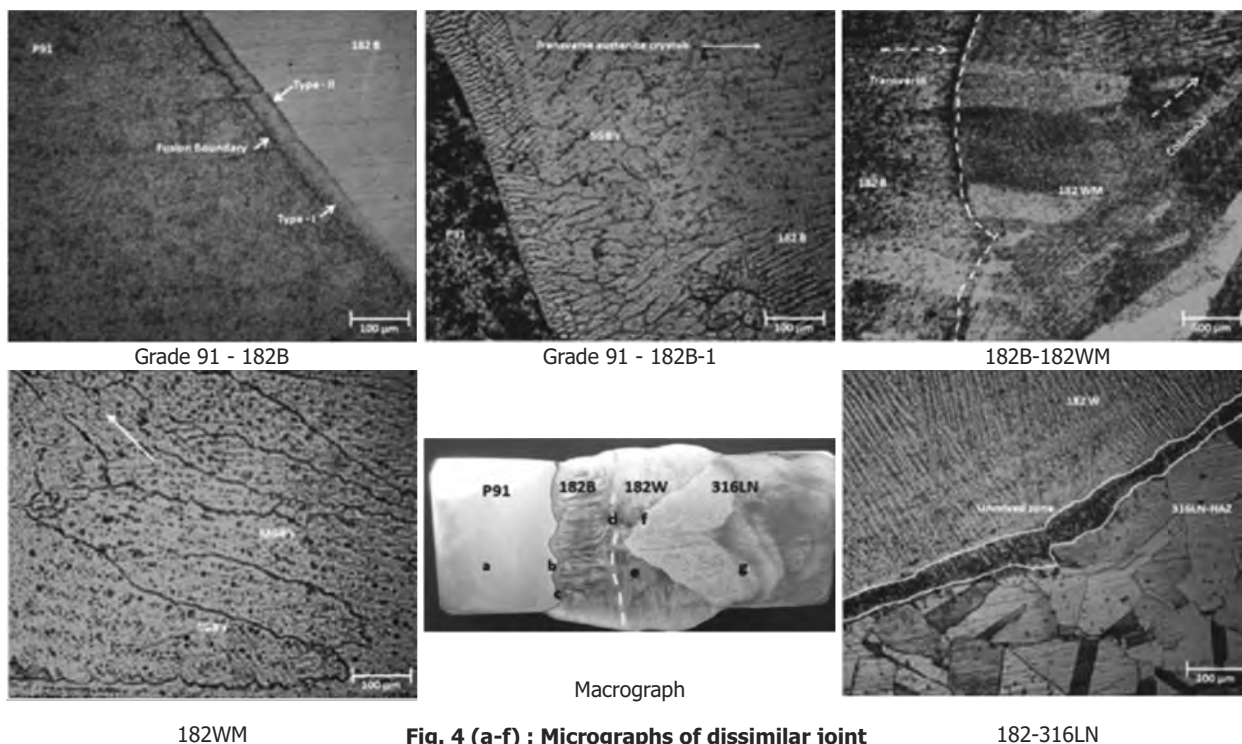


**Fig. 4 (a-f) : Micrographs of dissimilar joint**

The macrostructure of the dissimilar joint is shown in **Fig. 4a** which is free from macro level defects. The average width of buttering layer is about 6 mm and the grains are grown in the transverse direction. A clear interface was observed between grade 91 and Inconel 182 buttering layer. Moreover, transition region was also observed between Inconel 182 buttering and Inconel 82/182 welding. The micrographs of various regions of dissimilar joint are shown in **Fig. 4**, and the macrograph is also included. In **Fig. 4a**, regions like buttering and welding are clearly visible. The optical micrographs of the interface region

between grade 91 to 182 buttering are shown in **Fig. 4b**. From this micrograph, along with the fusion boundary, Type-I and Type-II boundaries are also visible [1]. The formation of these boundaries is due to the change in primary mode solidification (ferritic to austenitic). In **Fig. 4c**, transverse austenite crystal was oriented across the DMJ, and the second phase particles are segregated at the grain boundaries. In addition to that, Solidification grain boundaries (SGB's) are also visible. The interface between Inconel 182 buttering and 82/182 welding is shown in **Fig. 4d**. From this, a clear transition of transverse to

columnar dendrites was visible. This transition occurred mainly because of change in the direction of weld cooling [8]. The optical micrograph of 182 weld metal is shown in Fig. 4e which consists of austenite grains oriented towards the direction of weld cooling. The interface between Inconel weld metal and SS 316LN-BM is shown in Fig.4f. The unmixed zone was observed in the micrograph and this is due to the excess melting of base metal and resolidified without filler metal.

### 3.2 Microhardness Variation across the Dissimilar Joint

Microhardness variation profile across the dissimilar joint is shown in Fig. 5. The hardness measurements were taken at the top, middle and bottom of the joint. A non-uniform hardness profile was observed along the DMJ. The hardness values of grade 91 and SS316LN base metals are in a range of 240-260 HV and 210-245 HV. A sudden dip in the hardness was observed approximately 4 mm from the fusion interface, and then it is increased. The hardness at the interface of grade 91 and 182 buttering was about 260HV this may be due to the carbon migration from the grade 91 side to 182 buttering side and the sudden cooling rate during the welding. Both buttering and welding are carried out using same filler, so there are no appreciable variations in the hardness in these regions. The hardness in the HAZ of SS316LN side is slightly increased compared to its adjacent region. This may be due to the element migration from the weld metal to the SS316LN side and repeated tempering results in grain refinement which leads to the increase in hardness [9]. From the hardness survey, it is concluded that the weakest region in the dissimilar joint is located at 4mm from the interface of grade 91 to 182 buttering.

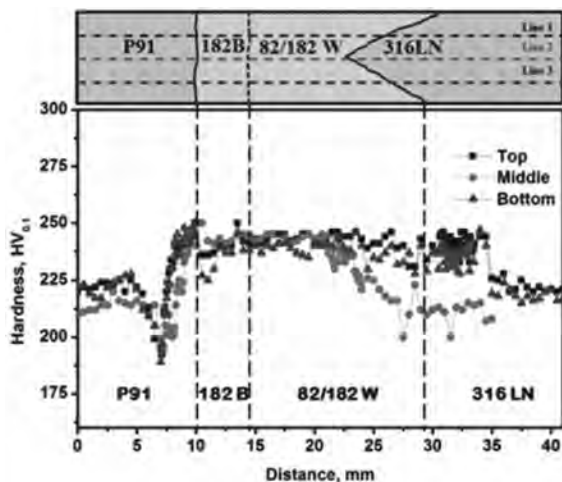
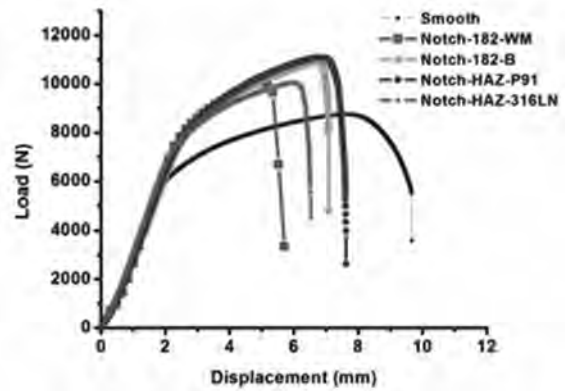


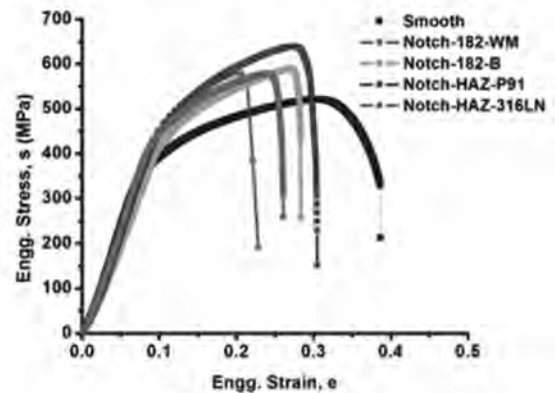
Fig. 5 : Microhardness distribution profile across the dissimilar joint

### 3.3 Tensile Properties

Fig. 6 shows the load-displacement and their corresponding stress-strain curves for various regions of dissimilar joint. Totally, three specimens were tested for each case and the average values are reported in Table 1.



(a) Load-displacement curve



(b) Engg. stress-strain curve

Fig. 6 (a-b) : Tensile curves for different regions of dissimilar joint

The base metals tensile properties are also included for comparison. The transverse tensile specimens were failed on the P91 side which is approximately 4.5 mm from the P91 to Inconel 182 buttering interface. These results are in good agreement with the hardness variation of dissimilar joint. The transverse tensile specimens were failed at the lowest hardness distributed region. Among the different regions of dissimilar joint, the HAZ of grade 91 side exhibits higher notch tensile strength compared to other regions due to the presence of hard zone formed adjacent to the interface of grade 91 due to the carbon migration. Notch tensile strength for buttering region is higher compared to weld metal. Even though it has a similar chemical composition, the base metal dilution is high for

**Table 1 : Tensile properties of different regions of dissimilar joint**

	0.2% Yield Strength (MPa)	Ultimate tensile strength (MPa)	Elongation in 25 mm gauge length (%)	Reduction in cross sectional area (%)	Notch tensile strength (MPa)	Location of Failure
P91-BM	590	720	19	55	1090	---
SS316LN-BM	312	590	44	63	707	---
Transverse	394	519	9	82	---	P91 BM
Notch in Weld metal	---	---	---	---	580	---
Notch in Buttering	---	---	---	---	590	---
Notch in HAZ-P91	---	---	---	---	638	---
Notch in HAZ-316LN	---	---	---	---	577	---

buttering region and the grains were oriented along the loading direction. So the strength is moderately higher compared to weld metal. The lowest notch tensile strength is observed for HAZ of 316LN. From the tensile test results, it is understood that the strength mainly depends upon the local microstructural features developed during welding and the grain orientation.

**3.4 Impact Toughness**

**Fig. 7** shows the variation of impact toughness of different regions of dissimilar joint.

The orientation of the notch is placed in the thickness direction of the weld. In all cases, the toughness values are greater than the prescribed value of 80 J [10]. This minimum prescribed value is framed for U notch specimens, but in the present investigation, V notch was used, and the V-notch is having higher stress concentration effect than U notch specimens.

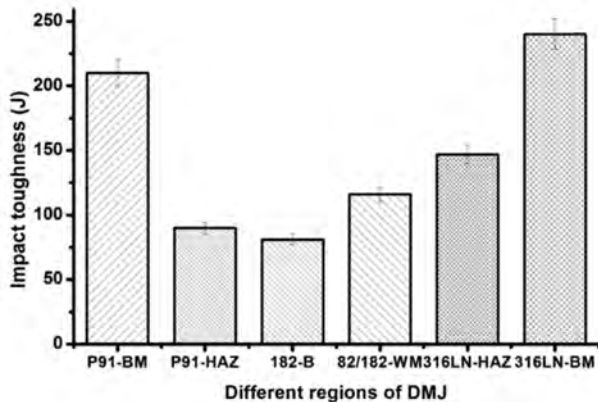


**Fig. 7 : Impact toughness variations of different regions of DMJ**

Hence the values produced by V notch are slightly lower than U notch specimens. Among the different regions, the HAZ of grade 91 side yielded lowest toughness value and this may due to complex microstructure developed at the interface. This value is having good agreement with microhardness survey of dissimilar joint. In the region, close to the fusion interface of grade 91 side exhibits higher hardness compare to its base metal, so the energy absorbed in this region is lower. Toughness values of Inconel 182 buttering and Inconel 82/182 are 81 and 116 J respectively. This variation in the toughness values arises mainly because of the grain orientation.

**3.5 SEM Fractographs**

The fracture surfaces tested under tensile load are shown in **Fig. 8**.

Low magnification image of the smooth specimen is shown in **Fig. 8a**. The width and thickness of the specimens are significantly reduced to 3.4 mm and 0.8 mm respectively. This shows that before failure, the specimen is observed to be subjected to more energy. High magnification fracture surface (**Fig. 8b**) consists of fine equiaxed dimples. The fracture pattern was very similar to that of base metal because it fails at the interface between HAZ to BM. Fractographs of buttering and weld metal is shown in **Fig. 8 (c-f)** in which the fracture was dominated by ductile dimples and teat ridges, and some of the precipitate particles are also visible, in both, the fracture surfaces some deep cavities are presented. The volume fraction of ductile dimples in weld metal is more compared to buttering. In **Fig. 8(g-h)**, the fracture surface consists of shallow dimples and some flat facets. Fractographs of HAZ of 316LN side is shown in **Fig. 8(i-j)** which comprise of large

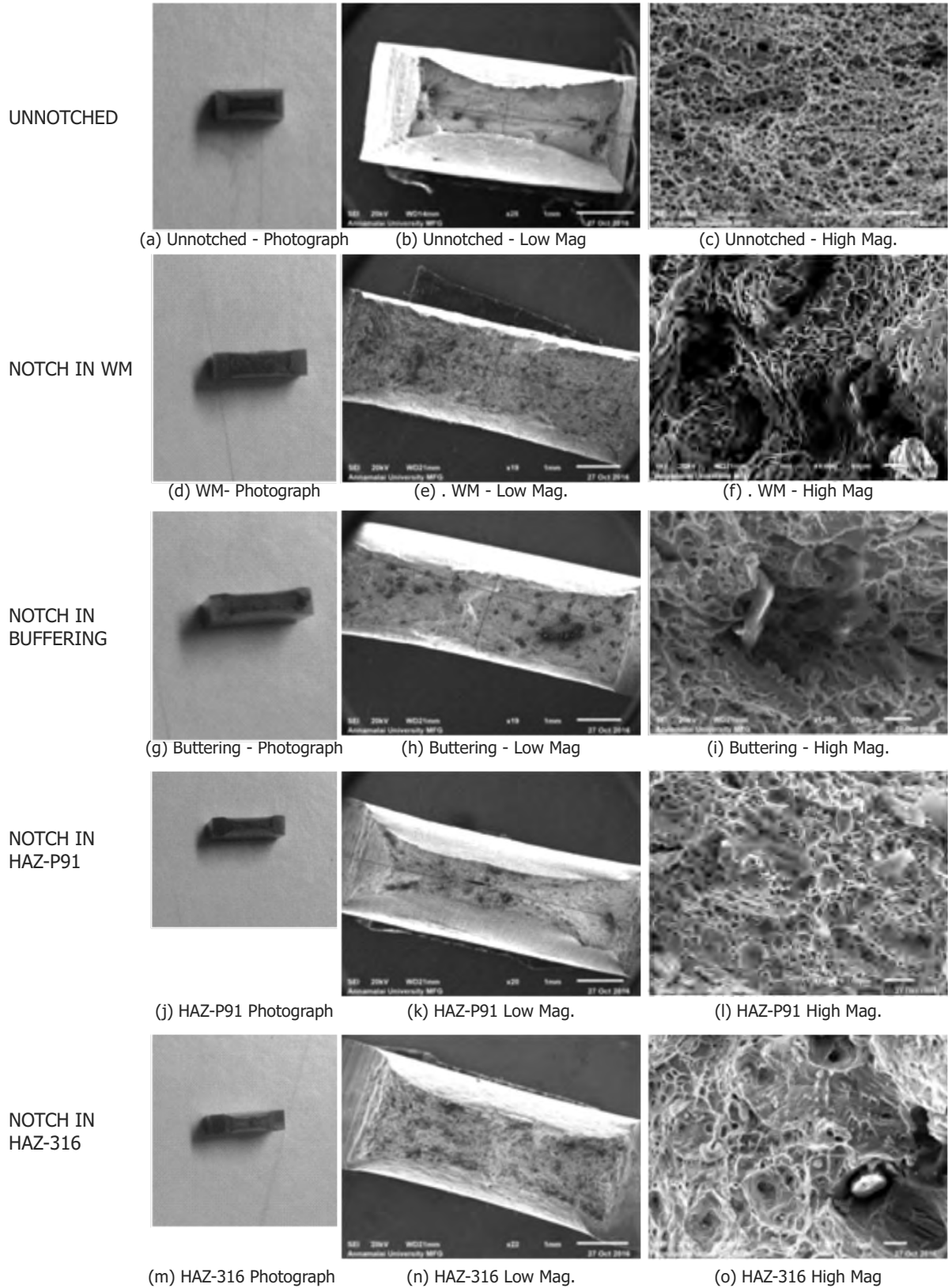


**Fig. 8 (a-o) : SEM-Fractographs of tensile specimens**

dimples surrounded by tear ridges, and the secondary phase particles are also visible which acts as a crack initiator during tensile testing.

The fracture surfaces of Charpy impact specimens of various regions of dissimilar joint are shown in **Fig. 9(a-h)**. All the fracture surfaces are failed in a ductile mode which is evidenced by dimples and tear ridges.

By visualizing the low magnification fracture surface, the lateral contraction was observed in the midsection whereas lateral expansion was visible at the toe end, so all the specimens show ductile nature. The HAZ of 316LN side shows highest impact toughness compare to other regions. Impact toughness of weld metal is slightly higher than buttering region because of the orientation of austenite crystals.

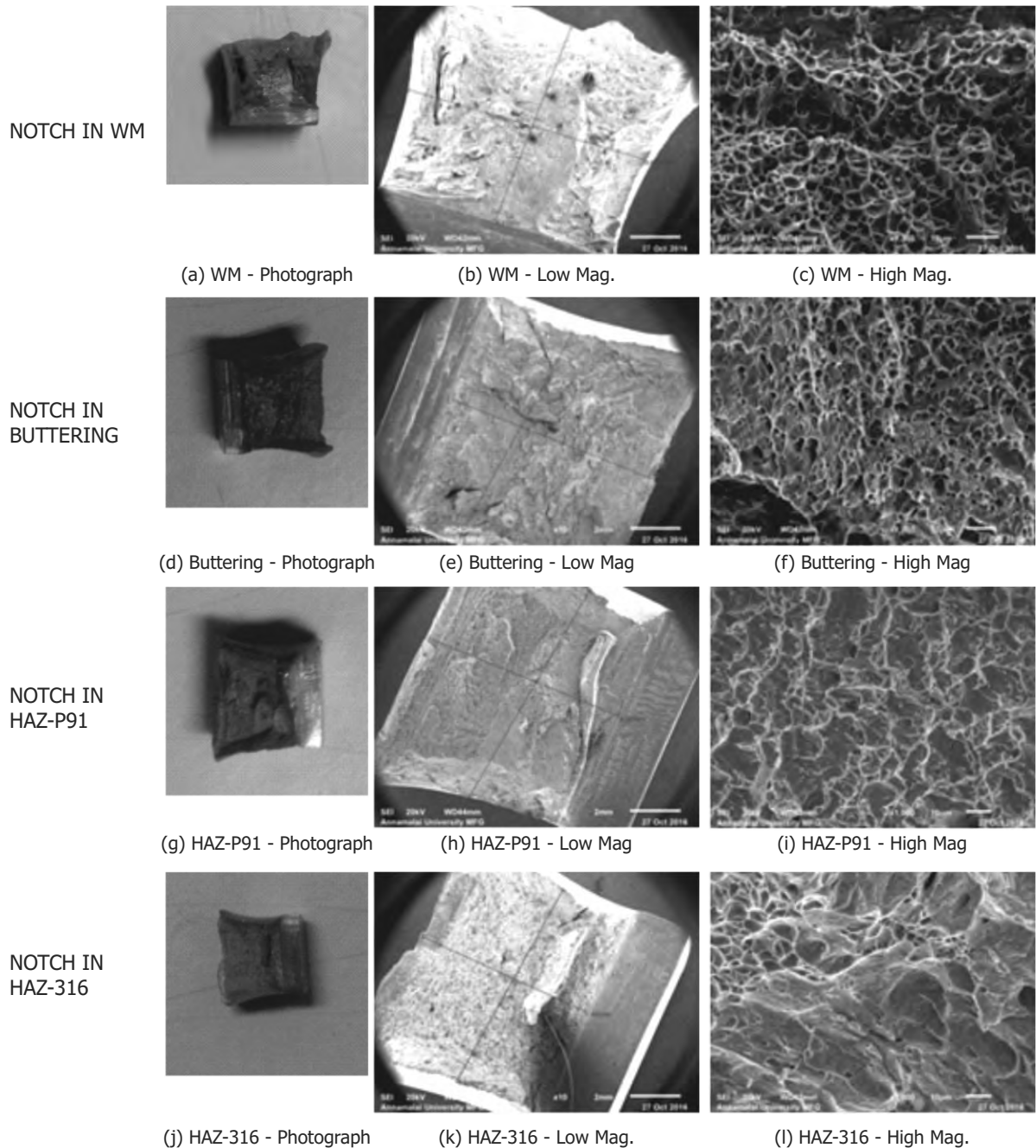


**Fig. 9 (a-l) SEM-Fractographs of charpy V notch impact specimens**

#### 4.0 CONCLUSIONS

1. The weld metal microstructure consists fully austenite crystal oriented towards the direction of cooling. The formation of type-I and type-II boundaries are the result of change in primary mode solidification and it is observed near to the fusion interface between buttering and grade 91-BM. The formation of unmixed zone is a result of total melting and resolidified without filler metal.
2. A complex hardness profile was observed across the dissimilar especially at the interface. Lowest hardness is observed approximately at 4 mm from the interface between Inconel 182 buttering and P91 base metal.
3. The cross weld tensile specimens were failed at the outer edge of the HAZ of grade 91 side with a lower tensile strength than P91-BM. Among the different regions of dissimilar joint, the HAZ of grade 91 steel yielded higher notch tensile strength.
4. All the Charpy specimens are failed in ductile mode. Lateral expansion and contraction are visible through low magnification fracture surfaces. The toughness values are less than the base metals, but it exceeds minimum prescribed value of 80J.

#### ACKNOWLEDGEMENTS

The authors are grateful to UGC-DAE-CRS consortium for providing financial assistance to carry out this investigation (Project No. CSR-KN/CRS-56/2013-14/655). Authors wish to express their sincere thanks to M/s. Mailam India Pvt. Limited, Pondicherry for supplying filler metals.

#### REFERENCES

- [1] Karthick K, Malarvizhi S, Balasubramanian V, Krishnan SA, Sasikala G and Albert SK (2017); Tensile properties of shielded metal arc welded dissimilar joints of nuclear grade ferritic steel and austenitic stainless steel, *Journal of the Mechanical Behavior of Materials*, 25(5-6), pp.171-178.
- [2] Teemu S, Matias A, Roman M, Pekka N, Päivi KR, Ulla E and Hannu H (2016); Microstructural, mechanical, and fracture mechanical characterization of SA 508-Alloy 182 dissimilar metal weld in view of mismatch state, *International Journal of Pressure Vessels and Piping*, 145, pp.13-22.
- [3] Jang C, Lee J, Sung KJ and Eun JT (2008); Mechanical property variation within inconel 82/182 dissimilar metal weld between low alloy steel and 316 stainless steel, *International Journal of Pressure Vessels Piping*, 85(9), pp.635-646.
- [4] Kim JW, Lee K, Kim JS and Byun TS (2009); Local mechanical properties of alloy 82/182 dissimilar weld joint between SA508 Gr.1a and F316 SS at RT and 320°C, *Journal of Nuclear Materials*, 384(3), pp. 212-221.
- [5] Pandey S, Prasad R, Singh PK and Rathod DW (2014); Investigation on dissimilar metal welds of SA312 type 304LN pipe (extruded) and SA508Gr.3Cl.1 pipe (forged), Bhabha Atomic Research Centre, Mumbai, India, Report No. 2008/36/107-BRNS/4038A.
- [6] Zhang ZL, Hauge M, Thaulowa C and Ødegård J (2009); A notched cross weld tensile testing method for determining true stress-strain curves for weldments, *Engineering Fracture Mechanics*, 69(3), pp.353-366.
- [7] Wendell B, Jones CR, Hills D and Polonis H (1991); Microstructural evolution of modified 9Cr-1Mo steel, *Metallurgical Transactions A*, 22, pp.1049-1058.
- [8] Wang HT, Wang GZ, Xuan FZ, Liu CJ, Tu ST (2014) Local mechanical properties of a dissimilar metal welded joint in nuclear power systems, *Materials Science and Engineering: A*, 568, pp.108-117.
- [9] Rathod DW, Pandey S, Singh PK and Prasad R (2015); Mechanical properties variations and comparative analysis of dissimilar metal pipe welds in pressure vessel system of nuclear plants, *Transactions of the ASME, Journal of Pressure Vessel Technology*, 138(1), pp. 011403-011409.
- [10] IGCAR, Prototype fast breeder reactor specification for the qualification of the welding consumables, Indira Gandhi Centre for Atomic Research, Kalpakkam, India, Report No. PFBR/32040/SP/1002/R-0.